Hydrogen-isotope motion in scandium studied by ultrasonic measurements

R. G. Leisure
Department of Physics, Colorado State University, Fort Collins, Colorado 80523

R. B. Schwarz and A. Migliori
Los Alamos National Laboratory, Los Alamos, New Mexico 87545

D. R. Torgeson
Ames Laboratory, Iowa State University, Ames Iowa 50011

I. Svare
Department of Physics, University of Trondheim, NTH, N-7034 Trondheim, Norway
(Received 1 March 1993)

Resonant ultrasound spectroscopy has been used to investigate ultrasonic attenuation in single crystals of Sc, $ScH_{0.25}$, and $ScD_{0.18}$ over the temperature range of 10–300 K for frequencies near 1 MHz. Ultrasonic-attenuation peaks were observed in the samples containing H or D with the maximum attenuation occurring near 25 K for $ScH_{0.25}$ and near 50 K for $ScD_{0.18}$. The general features of the data suggest that the motion reflected in the ultrasonic attenuation is closely related to the low-temperature motion seen in nulcear-magnetic-resonance spin-lattice-relaxation measurements. The ultrasonic results were fit with a two-level-system (TLS) model involving tunneling between highly asymmetric sites. The relaxation of the TLS was found to consist of two parts: a weakly temperature-dependent part, probably due to coupling to electrons; and, a much more strongly temperature-dependent part, attributed to multiple-phonon processes. The strongly temperature-dependent part was almost two orders of magnitude faster in $ScH_{0.25}$ than in $ScD_{0.18}$, in accordance with the idea that tunneling is involved in the motion. Surprisingly, the weakly temperature-dependent part was found to be about the same for the two isotopes. The asymmetries primarily responsible for coupling the TLS to the ultrasound are attributed to interactions between hydrogen ions that lie on adjacent c axes. The results are consistent with an isotope-independent strength for the coupling of the TLS to the ultrasound.

I. INTRODUCTION

Features of the rare-earth–metal-hydrogen systems $RH(D)_x$ (R =Sc,Y,Ho,Er,Tm,Lu) have attracted much attention. In marked contrast to most metal-hydrogen systems, H and D are not precipitated into a hydride phase as the temperature is lowered, but remain in solid solution,[1] even for x as high as 0.2–0.3. It has been established[2] that hydrogen ions occupy the tetrahedral (T) sites in the hcp metal lattice with little or no occupancy of the octahedral (O) sites. Ordering of the hydrogen on the interstitial sites occurs as the temperature is lowered. Hydrogen (deuterium) pairs are formed which involve occupancy of the second-nearest-neighbor T sites along the c axis with a bridging metal atom in a H-R-H configuration. The pairs form chains[3,4] along the c axis with some correlation[5,6] between chains. These features are illustrated in Fig. 1. Figure 1(a) shows the hcp crystal structure, and the axis of symmetry indicates *one* of the lines of tetrahedral sites. Similar lines, of course, pass through each metal atom. Figure 1(b) shows a cross section of the hcp lattice parallel to the c axis. A pair of occupied T sites with a bridging metal atom is illustrated in Fig. 1(b) by sites 1 and 2. The two closely spaced T sites such as 3 and 4 are not simultaneously occupied. Finally, Fig. 1(c) depicts the chainlike ordering of pairs along the c axis, which has been proposed to account for neutron-scattering results.[4,7]

The dynamical properties of these materials have been investigated using various experimental techniques. Neutron-scattering measurements[8,9] show that hydrogen in the T sites vibrates in a highly anisotropic and anharmonic potential. Diffusive motion involves both a long-range and a local motion. The relatively slow, rate-limiting, motion responsible for long-range diffusion[10–12] involves T-O-T jumps, labeled I in Fig. 1(b), with an activation energy of approximately 0.6 eV. A motion with approximately the same activation energy has been observed in low-frequency internal friction measurements.[13] Whereas the long-range motion appears to be well understood, the local motion is somewhat puzzling. Quasielastic-neutron-scattering (QNS) experiments show a very fast local motion between nearest-neighbor T sites in YH_x (Ref. 14) and ScH_x (Ref. 15), labeled II in Fig. 1(b). NMR proton-spin-lattice-relaxation measurements[16] in ScH_x and YH_x indicate a fast local motion, also assumed to involve jumps between nearest-neighbor T sites lying along the c axis. The relation between the two types of local motion is unclear; they occur over the same temperature range, but the QNS-derived rates are at least 100 times faster than the NMR-derived rates. The temperature dependence of the two rates is also quite different.

A theoretical attempt has been made to reconcile the two very different results for local motion with a model involving tunneling between nearest-neighbor T sites with a wide range of asymmetries which strongly influences the tunneling transition rates.[17] Tunneling of H trapped near O has also been invoked[18] to explain acoustic measurements on YO_yH_x. An excellent test for tunneling is to measure its isotope dependence, since the tunneling matrix element depends strongly on the mass of the tunneling entity. Unfortunately, NMR experiments are strongly influenced by the electric quadrupole moment of deuterium, and neutron scattering also differs markedly for the two isotopes. Ultrasound responds in the same way to the different isotopes and thus is an excellent tool to study such effects.[19–21] In addition, ultrasonic experiments on *single crystals* have the potential for yielding information about the H-H interactions responsible for the attenuation peaks. In view of these considerations, we decided to perform ultrasonic measurements on ScH_x and ScD_x. A preliminary account of these measurements has been given elsewhere.[22]

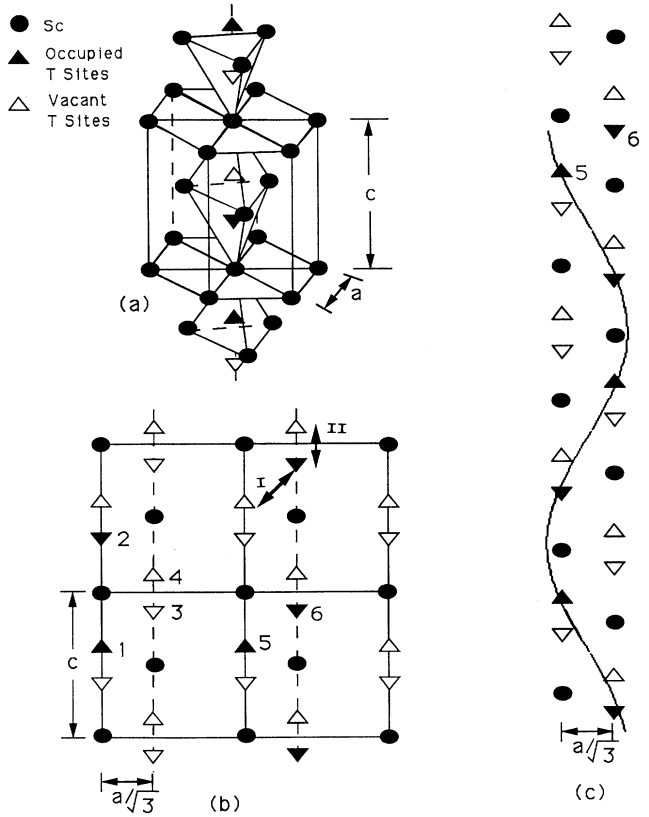

FIG. 1. (a) Crystal structure of α-phase $ScH(D)_x$ showing hcp metal atoms and one line of tetrahedral sites. Similar lines pass through each metal atom. (b) Cross section of the $ScH(D)_x$ lattice. Hydrogen sites and jump processes are described in the text. (c) Chainlike structure proposed to explain neutron-scattering results.

II. EXPERIMENTAL DETAILS

Scandium single crystals were grown at the Ames Laboratory, Iowa State University. Rectangular parallelepipeds, ≈ 2 mm on an edge, were cut from larger single-crystal samples using an electric discharge machine. Hydrogen or deuterium was loaded from the gas phase as described in Ref. 9, and the amount absorbed was determined by the weight gain. Results are reported below on three samples: Sc, $ScD_{0.18}$, and $ScH_{0.25}$. The room-temperature dimensions of these three samples in mm were, respectively, $1.80 \times 1.89 \times 2.36$, $1.51 \times 1.77 \times 2.00$, and $1.59 \times 1.80 \times 1.97$. In each case one axis of the parallelpiped lay along the crystalline c axis to within 0.5°. For the Sc sample the short axis of the parallelepiped was along the c axis, while for the other two samples the long axis of the parallelepiped was along the c axis. Because a crystal of hexagonal symmetry is elastically isotropic in the basal plane, the orientations of the other crystalline axes relative to the parallelepiped were not determined.

Resonant ultrasound spectroscopy[23] was used to measure the ultrasonic attenuation. With this technique a single-crystal rectangular-parallelepiped sample is placed corner to corner between two piezoelectric transducers; one transducer is used for the generation and the other for the detection of ultrasonic vibrations. By sweeping the excitation frequency, a large number of the lowest-frequency vibrational eigenmodes of the sample can be measured at a constant temperature. As an illustration, a segment of the frequency spectrum for a $ScD_{0.18}$ single-crystal parallelepiped is shown in Fig. 2. From such a spectrum of eigenfrequencies, a complete set of elastic constants can be determined. For each of the samples, we have identified about 30 of the lowest-frequency eigen-

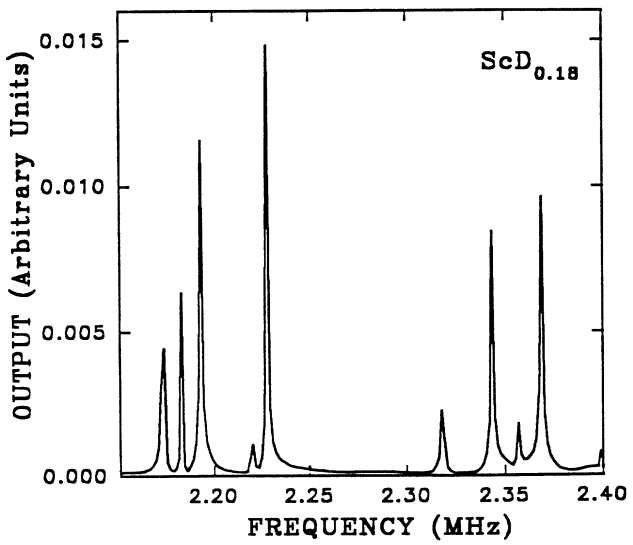

FIG. 2. Section of a resonant ultrasound frequency spectrum of a single-crystal ScD_x parallelepiped showing several vibrational eigenmodes. The widths of many such eigenmodes were measured as a function of temperature to derive the ultrasonic loss.

modes by fitting our measured frequencies to a set of elastic constants using the method described by Visscher *et al.*[24] In general, each of the vibrational eigenmodes depends on a combination of elastic constants. However, the lowest eigenfrequency and a few of the higher eigenfrequencies depend on only one or two elastic constants. This fact enables us to obtain a rather accurate description of the temperature dependence of some of the elastic constants by simply measuring the temperature dependence of a selected number of eigenfrequencies. In addition, the ultrasonic attenuation associated with such eigenfrequencies is obtained from these measurements. In the present study the emphasis is on the temperature dependence of the ultrasonic loss, which is obtained from the inverse of the Q of the eigenmodes. Those modes which depend on only one or two elastic constants are particularly useful for making a microscopic interpretation of the phenomena responsible for the ultrasonic loss.

III. RESULTS

Figure 3 shows results for the ultrasonic loss $1/Q$ for two *different* vibrational eigenmodes in $ScD_{0.18}$. Our analysis shows that the two modes of Fig. 3 depend only on the shear elastic constants C_{44} and C_{66}; that is, the derivative of the computed eigenfrequency with respect to the elastic constants is zero for the other three elastic constants. Further, the lower-frequency mode, at 0.73 MHz, is almost pure C_{44}; the dependence of the higher-frequency mode, at 1.01 MHz, on elastic constants is weighted about 40% C_{44} and 60% C_{66}. There are three main features shown in Fig. 3. First, there is some evidence of an ultrasonic-attenuation anomaly near 170 K, in the temperature range where resistance anomalies have been observed and associated with hydrogen ordering.[25] The attenuation anomalies in this temperature range were found to depend on the rate and direction of temperature change and have not been well characterized.

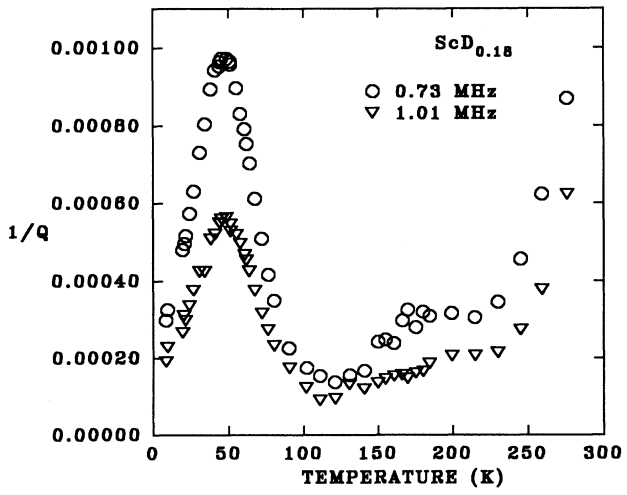

FIG. 3. Ultrasonic loss $1/Q$ for two different vibrational eigenmodes in $ScD_{0.18}$. The mode at 0.73 MHz is almost pure C_{44}, whereas the mode at 1.01 MHz is about 40% C_{44} and 60% C_{66}.

Second, the loss increases as the temperature approaches room temperature; this increase is probably associated with the long-range diffusion process. Finally, the dominant effect is the broad loss peak with the maximum near 50 K. These results will be discussed in more detail below.

Figure 4 shows data for $ScH_{0.25}$ at three different frequencies. The solid lines are theoretical fits to the data to be described below. Figure 5 shows similar data for $ScD_{0.18}$. The different frequencies correspond to different vibrational eigenmodes. It is seen that the attenuation-peak position shifts little, if any, with a change in measuring frequency. The attenuation peak for $ScD_{0.18}$ occurs at a considerably higher temperature than is the case for $ScH_{0.25}$.

Measurements were also made on an undoped Sc crystal. There is no low-temperature peak in this case, only a small, almost temperature-independent, attenuation.

IV. DISCUSSION

We describe our results in terms of the theory of two-level systems (TLS's). An interstitial such as hydrogen, which may occupy either of two nearby interstitial sites, can be described as a two-level system with an energy splitting $E=(E_T^2+A^2)^{1/2}$, where E_T is the tunnel splitting and A is the difference in energy of the two wells (asymmetry). This formalism may be used even in cases where tunneling is not a factor, in which case we simply have $E_T=0$. The ultrasonic loss due to relaxation is given by[26]

$$\frac{1}{Q}=\frac{n_0 D^2}{4Ck_BT}\operatorname{sech}^2\left[\frac{E}{2k_BT}\right]\frac{\omega\tau}{1+\omega^2\tau^2}\ , \tag{1}$$

where n_0 is the concentration of TLS's, $D=\delta E/\delta\varepsilon$ is the variation of the energy-level splitting with respect to the ultrasonic strain ε, C is an elastic constant, $\omega/2\pi$ is the ultrasonic frequency, and τ is the relaxation time. It is usually the case[27] that $\delta A/\delta\varepsilon \gg \delta E_T/\delta\varepsilon$, so that

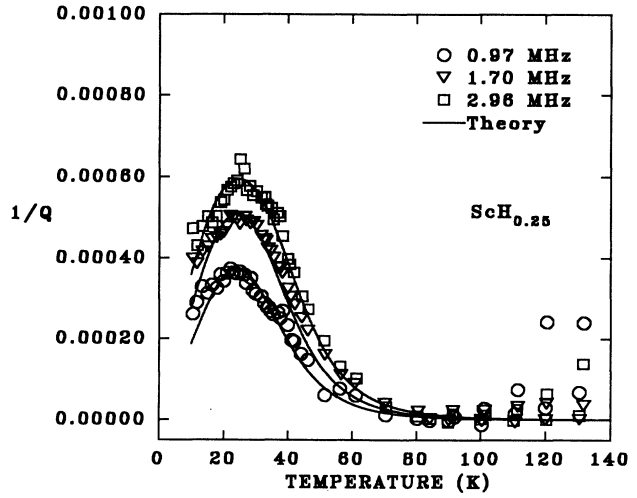

FIG. 4. Ultrasonic loss $1/Q$ for three different frequencies in $ScH_{0.25}$. The solid lines are fits to the data described in the text.

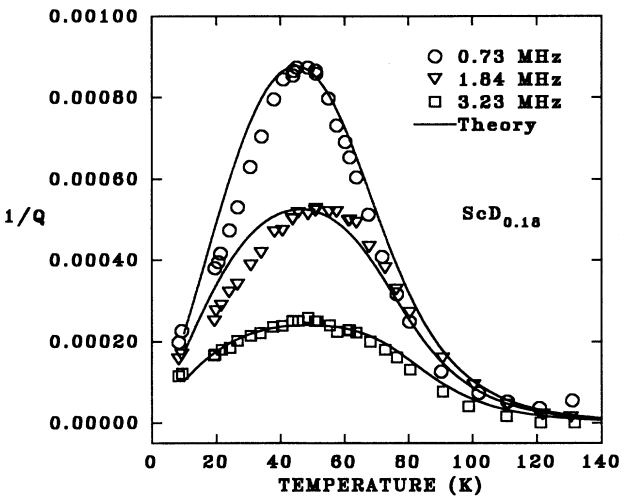

FIG. 5. Ultrasonic loss $1/Q$ for three different frequencies in $ScD_{0.18}$. The solid lines are fits to the data described in the text.

$$D=\frac{A}{E}\frac{\delta A}{\delta\varepsilon}=\gamma\frac{A}{E}\ . \tag{2}$$

We discuss below several features of the data in terms of Eq. (1): the dependence of the attenuation on the vibrational eigenmode, the temperature and frequency dependences of the data, and the magnitude of the attenuation. First, we address the dependence of the magnitude of the attenuation on vibrational eigenmode shown in Fig. 3. As discussed above, these two modes differ in their dependence on the two shear elastic constants C_{44} and C_{66}. The mode specific part of Eq. (1) is the factor D^2/C. We find that C, the elastic constant, is approximately the same for the two modes, i.e., $C_{44}\approx C_{66}$. Thus, from Eq. (2), we expect the difference in the maximum value of $1/Q$ to be due to $\delta A/\delta\varepsilon$, where ε is the ultrasonic strain associated with a particular vibrational eigenmode. As mentioned above, the lower-frequency mode in Fig. 3 depends solely on C_{44}. For a crystal of hexagonal symmetry, the elastic constant C_{44} is associated with a single strain ε_4 ($=\varepsilon_{yz}$ in tensor notation). This strain corresponds to an angular distortion in the yz plane. The higher-frequency mode depends on a mixture of C_{44} and C_{66}. In hexagonal symmetry C_{66} is associated with a single strain $\varepsilon_6=\varepsilon_{xy}$, an angular distortion in the basal plane. By symmetry, C_{44} is equivalent to C_{55}; thus, we also expect a distortion in the xz plane corresponding $\varepsilon_5=\varepsilon_{xz}$. In terms of the ultrasonic strains, the results of Fig. 3 may be summarized as follows: The pure shear strains ε_4 and ε_6 give rise to ultrasonic attenuation, and the attenuation associated with $\delta\varepsilon_4$ is larger than that associated with $\delta\varepsilon_6$. An analysis of several other vibrational eigenmodes supports the conclusion that the attenuation associated with $\delta\varepsilon_4$ is larger than that associated with $\delta\varepsilon_6$.

It seems reasonable to attribute the asymmetries represented by A to H-H (D-D) interactions. Since we have identified the vibrational eigenmodes, it is possible to obtain information about the nature of the asymmetries which contribute to $\gamma=\delta A/\delta\varepsilon$. It is important to note that, to first order in the strain, *neither* of the shear strains ε_{xz} or ε_{xy} involved in the measurements of Fig. 3 changes the separation of T sites lying along the same c axis. Therefore the loss peaks shown in Fig. 3 *do not* depend on a modulation of the separation of paired ions such as 1 and 2 in Fig. 1(b). Vibrational eigenmodes which depend on C_{33} will change the separation of such pairs. None of the modes identified depends purely on C_{33}, but several have a contribution from C_{33}. Those modes depending partially on C_{33} do not show an especially large loss peak. Thus there is no indication that the interaction between paired hydrogen ions such as 1 and 2 makes a major contribution to γ. Our interpretation of this result is that such pairs are effectively locked in place at the temperatures of our experiments and do not contribute to the attenuation because they are immobile on the time scale of the ultrasonic frequency. To account for the modulation of asymmetries which contribute to γ, we are led to look for interactions between adjacent c axes. The closest such T sites are those such as 5 and 6 in Figs. 1(b) and 1(c). These sites are about 2.36 Å apart. The identification of the interaction between these sites as being primarily responsible for the ultrasonic attenuation provides a qualitative explanation for the different magnitudes of the attenuation peaks in Fig. 3 because $\delta\varepsilon_4$ ($=\delta\varepsilon_{yz}$), the strain associated with C_{44}, is more effective in modulating this separation than is $\delta\varepsilon_6$ ($=\delta\varepsilon_{xy}$), the strain associated with C_{66}. An interaction between sites of types 5 and 6 appears to be necessary to support the type of chain formation illustrated in Fig. 1(c). Such interactions would not lead to ultrasonic attenuation for T sites *within* a chain, because such sites would be locked in pairs. However, sites at the ends of chains, as illustrated in Fig. 1(c), could be responsible for ultrasonic attenuation. The ultrasonic attenuation in $YD_{0.10}$ was attributed to the same type of interaction.[28]

We now turn to a description of the temperature and frequency dependence of the attenuation peaks. Frequently, ultrasonic-attenuation peaks are described mainly by the temperature dependence of τ, which is often due to thermally activated classical hopping. The present case is more complicated. First, it seems unlikely that classical hopping over a barrier is responsible for the relaxation. From neutron-scattering measurements, the optical frequency of hydrogen ions in the T sites is $\approx 2\times 10^{13}$ Hz. If we assume that the attenuation peaks correspond to $\omega\tau\approx 1$ and use the optical frequency as the attempt frequency, then the activation energy required to give attenuation peaks at the observed temperatures is ≈ 30–60 meV for the two isotopes, less than the energy of the first excited state of the hydrogen ions in the T sites.[9,29] As will be discussed below, it appears that the results correspond to $\omega\tau<1$, so that an even smaller activation energy would be required. Because the classical activation energies required to fit the data are in conflict with the neutron-scattering experiments and since such low apparent values of activation energies are often an indication of quantum-mechanical tunneling,[30] we describe the relaxation in terms of tunneling between nearby interstitial sites. The interpretation of our results is quite

different from a classical Debye relaxation peak in at least two ways: the relaxation time τ is not due to classical barrier hopping, and the factor $\mathrm{sech}^2(E/2k_BT)$ is very important, with the result that the peak of the attenuation does not correspond to $\omega\tau=1$.

In applying Eq. (1) to our results, we assume that A is described by a distribution resulting from interactions between neighboring hydrogen ions. Because of the crystalline nature of the host, we assume that E_T is single valued. Such a model, with a wide distribution of asymmetries, was used[17] to describe the NMR spin-lattice relaxation in ScH_x. We find that the parameters of Ref. 17 give a reasonably good fit to the present $ScH_{0.25}$ data, which supports the idea that the motion seen in the present experiments is similar to that seen by NMR. However, we have not been able to achieve a good fit to the $ScD_{0.18}$ data with a reasonable extension of the ScH_x parameters. Thus we adopted the approach described below.

Equation (1) must be integrated over an appropriate distribution of asymmetries using proper expressions for the relaxation time τ, which in general depends on the asymmetry. Relaxation of the TLS occurs as a result of coupling to electrons[31–35] and phonons.[17,20,36] In general, the electron and one-phonon rate are slowly varying functions of temperature, while the multiple-phonon rates are much more strongly dependent on temperature. The electron coupling in metals dominates the one-phonon coupling except possibly at very high asymmetries.[17] Figures 4 and 5 show that the peak position shifts little, if at all, with a change in frequency. This fact suggests that $\omega\tau<1$ for many of the tunneling centers. With these considerations, the shape of the attenuation curves and the relative magnitudes of the results for $ScH_{0.25}$ and $ScD_{0.18}$ suggest a qualitative explanation of our results. For temperatures less than the maximum of the attenuation, the increasing thermal population of levels combined with the weakly temperature-dependent relaxation rate gives a contribution to the attenuation which increases with temperature. The slowly varying relaxation rate is probably due to coupling to electrons. For temperatures near the maximum of the attenuation, a much more strongly temperature-dependent relaxation rate becomes dominant and the rapid decrease of τ leads to the decrease in the attenuation in the $\omega\tau<1$ limit. The strongly temperature-dependent relaxation rate is much weaker for D than for H, as would be expected for a process involving tunneling. The surprising point is that the weakly temperature-dependent rate needed to fit the data is approximately *the same* for the two isotopes, with the assumption that $\gamma_H\approx\gamma_D$ and that the distribution of asymmetries is approximately the same.

We now give the details of fitting the data. For the weakly temperature-dependent rate, we have used an expression for relaxation due to the electrons,[17]

$$\frac{1}{\tau_{\mathrm{el}}}=\frac{\pi KE_T^2}{\hbar E}\coth\left[\frac{E}{2k_BT}\right], \tag{3}$$

where K is a dimensionless parameter representing the coupling to the electrons. For the strongly temperature-dependent rate, we use

$$\frac{1}{\tau_p}=F_1\frac{T^5}{E^2}+F_2T^7, \tag{4}$$

where F_1 and F_2 are adjusted to fit the data. The total relaxation rate used in Eq. (1) is just the sum of the two relaxation rates, $\tau^{-1}=\tau_{\mathrm{el}}^{-1}+\tau_p^{-1}$. Equation (4) approximates the E and T dependence[17] of the theoretical two-phonon processes in the low-temperature limit. However, we find that these expressions give a good fit to the data even outside the low-temperature limit.

Following Ref. 17, we used Gaussian distributions of asymmetries centered around $+A_1$ and $-A_1$ (since positive and negative asymmetries are equally likely) with widths A_0. To minimize the number of parameters, we used the same A_1 and A_0 for both $ScH_{0.25}$ and $ScD_{0.18}$, although the different concentrations would probably justify somewhat different values for the two samples. The tunneling matrix element only enters through the value of KE_T^2, and K is not determined separately. For the large values of A used, the values of F_1 and F_2 needed for the fit are insensitive to the value of E_T for any reasonable value of E_T. The temperature and frequency dependences of the theoretical curves are determined by the distribution of asymmetries, KE_T^2, F_1, and F_2. The fitted values of these parameters are given in Table I for both isotopes. As can be seen from Table I, the parameters are the same for the two isotopes with the exception of F_1 and F_2, which are 50 times stronger for H than for D.

Tunneling provides an explanation for the differences between F_1 and F_2 for the two isotopes. The two-phonon relaxation rates depend on a tunnel splitting squared, and the tunnel splitting is, of course, smaller for D than for H because of the larger mass. Our results indicate that the ratio of the splittings is $\approx(50)^{1/2}$. This value is near the value 10 estimated for Nb.[37] The fact that the value of KE_T^2 needed to fit the data is the *same* for the two isotopes is a puzzle. One would have expected this parameter to differ for the two isotopes by a comparable magnitude. We have no explanation for this behavior at this time.

TABLE I. Parameters used to fit the temperature and frequency dependence of the ultrasonic attenuation in $ScH_{0.25}$ and $ScD_{0.18}$. The asymmetries are described by Gaussian distributions centered at $\pm A_1$ with a width A_0.

	A_1/k_B	A_0/k_B	KE_T^2/k_B^2	F_1	F_2
$ScH_{0.25}$	105 K	70 K	0.0014 K^2	4000 $s^{-1}K^{-3}$	4×10^{-5} $s^{-1}K^{-7}$
$ScD_{0.18}$	105 K	70 K	0.0014 K^2	80 $s^{-1}K^{-3}$	8×10^{-7} $s^{-1}K^{-7}$

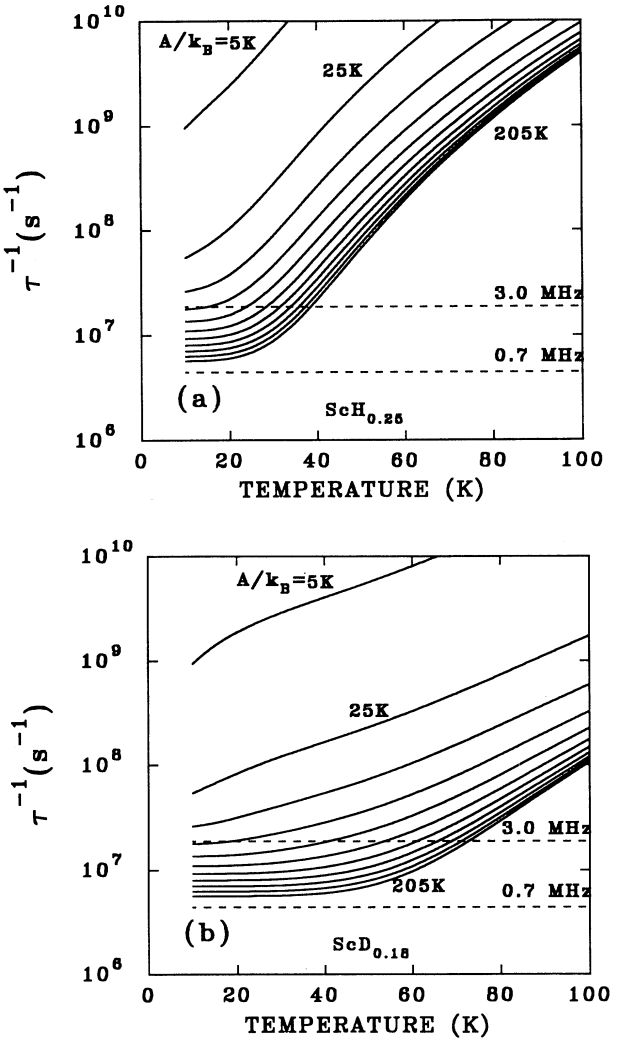

FIG. 6. Relaxation rate τ^{-1} used to fit the data, plotted as a function of temperature for several values of the asymmetry parameter A. The horizontal dotted lines correspond to $\tau^{-1}=\omega=2\pi f$ for the two different values of the frequency f shown in the figure. (a) $ScH_{0.25}$; (b) $ScD_{0.18}$.

The relaxation rates given by the parameters of Table I and used to fit the data are shown in Fig. 6(a) and 6(b) for a range of temperatures and asymmetries. These figures show that, over the temperature range of the peaks, the relaxation rate used to fit the $ScD_{0.18}$ data is roughly 50 times lower than the rate used to fit the $ScH_{0.25}$ data. Certain unusual features of the attenuation peaks are apparent in Figs. 6(a) and 6(b). The condition $\omega\tau=1$ is satisfied for only a fraction of the TLS's, those having relatively high asymmetries. For all cases in which $\omega\tau=1$ is satisfied, the condition $A<k_BT$ holds, so that the temperature dependence of the factor $\mathrm{sech}^2(E/2k_BT)$ in Eq. (1) plays an important role in the determination of the shape of the attenuation peaks. Those centers for which $\omega\tau<1$ make an important contribution to the attenuation for the following reason: Although the factor $\omega\tau/[1+(\omega\tau)^2]$ is relatively small for such centers, the factor $\mathrm{sech}^2(E/2k_BT)$ is relatively large.

We now turn to the magnitude of the attenuation. The two lower frequencies of Fig. 4 for $ScH_{0.25}$ each contain about 40% contribution from C_{44} and 60% contribution from C_{66} with only a small contribution from other elastic constants. Using our values of $C_{44}\approx C_{66}\approx 3\times10^{10}$ $\mathrm{N\,m^{-2}}$, we find $(n_0\gamma^2)_H=1.3\times10^{-12}$ $\mathrm{J^2\,m^{-3}}$ for the mode at 0.97 MHz and $(n_0\gamma^2)_H=1.0\times10^{-12}$ $\mathrm{J^2\,m^{-3}}$ for the mode at 1.7 MHz. With the present model, these two values should be the same; the agreement between the two results appears reasonable.

Figure 5 contains data and theoretical curves for $ScD_{0.18}$. As mentioned earlier, the curve at 0.73 MHz depends almost entirely on C_{44}. We find for this mode $(n_0\gamma^2)_D=1.8\times10^{-12}$ $\mathrm{J^2\,m^{-3}}$. The mode at 1.84 MHz contains contributions from several modes with about 40% each from C_{44} and C_{66}. We estimate $(n_0\gamma^2)_D\approx6\times10^{-13}$ $\mathrm{J^2\,m^{-3}}$ for this mode. Consistent with the earlier discussion, the value for the pure C_{44} mode is highest.

We were able to make a comparison between the results for $ScH_{0.25}$ and $ScD_{0.18}$ at a frequency of 1.71 MHz for almost identical eigenmodes. Details are given in Tables II and III. We find $(n_0\gamma^2)_H=6.5\times10^{-13}$ $\mathrm{J^2\,m^{-3}}$ and $(n_0\gamma^2)_D=4.7\times10^{-13}$ $\mathrm{J^2\,m^{-3}}$. It is interesting to note that $(n_0\gamma^2)_H/(n_0\gamma^2)_D=1.38$ is approximately equal to $\frac{25}{18}$, the ratio of the isotope concentrations for the two samples. This evidence for a linear dependence on concentration is too indirect to be anything more than suggestive. A linear dependence on concentration is *not* expected[38,39] for the usual Zener-type relaxation involving random occupancy of the interstitial sites. In contrast, a linear dependence is consistent with the model proposed above for coupling between the TLS and ultrasonic vibrations.

We have used the parameters of Table II for $ScH_{0.25}$ to calculate the NMR spin-lattice-relaxation rate for protons by integrating Eq. (19) of Ref. 17 over the Gaussian distribution of asymmetries. These parameters give a good description of the temperature dependence of the

TABLE II. Values of $n_0\gamma^2$ used to fit the magnitude of the attenuation in $ScH_{0.25}$ for various modes. The ultrasonic loss data for the mode at 1.71 MHz are not shown: Loss data for the other modes are shown in Fig. 4. The value of $|\gamma|$ was estimated under the assumption that n_0 is equal to 10% of the H ions.

Mode	37% C_{44}, 56% C_{66}	37% C_{44}, 56% C_{66}	38% C_{44}, 58% C_{66}, 4% C_{33}
Frequency (MHz)	0.97	1.70	1.71
$n_0\gamma^2$ ($\mathrm{J^2\,m^{-3}}$)	7.5×10^{-13}	6.5×10^{-13}	6.5×10^{-13}
$\lvert\gamma\rvert$ (eV)	0.17	0.16	0.16

TABLE III. Values of $n_0\gamma^2$ used to fit the magnitude of the attenuation in $ScD_{0.18}$ for various modes. The ultrasonic loss data for the mode at 1.71 MHz are not shown: Loss data for the other modes are shown in Fig. 5. The value of $|\gamma|$ was estimated under the assumption that n_0 is equal to 10% of the D ions.

Mode	92% C_{44}, 8% C_{66}	40% C_{44}, 40% C_{66}, 16% C_{33}	40% C_{44}, 54% C_{66}, 6% C_{33}
Frequency (MHz)	0.73	1.84	1.71
$n_0\gamma^2$ (J^2m^{-3})	1.2×10^{-12}	3.8×10^{-13}	4.7×10^{-13}
$\|\gamma\|$ (eV)	0.25	0.14	0.16

proton spin-lattice-relaxation rate. In addition, the magnitude of the relaxation rate is correctly described if we assume that 10% of the protons contribute to the low-temperature spin-lattice relaxation. (Reference 17 fit the results with 7% of the protons contributing; our somewhat higher value is due to a wider distribution of asymmetries used in the present calculation.) The agreement indicates that essentially the same motion is seen in the NMR and ultrasonic experiments; the present interpretation is essentially the same as that of Ref. 17.

To estimate $|\gamma|$ we assume that n_0 is proportional to the total hydrogen concentration. Our arguments above imply that only a small fraction of the hydrogen ions contribute to the attenuation. We will use the 10% figure to estimate $|\gamma|$. For the two lower-frequency modes of Fig. 4 which have nearly the same dependence on elastic constants (37% contribution from C_{44} and a 56% contribution from C_{66}), we find $|\gamma_H|=0.17$ eV for the mode at 0.97 MHz and 0.16 eV for the mode at 1.7 MHz. From Fig. 5 we find $|\gamma_D|=0.25$ eV for the mode at 0.73 MHz (almost pure C_{44}) and 0.14 eV for the mode at 1.84 MHz (16% C_{33}, 42% C_{44}, and 38% C_{66}). Finally, for a mode where a direct comparison of H and D is possible for the same eigenmode ($\approx$39% C_{44}, 56% C_{66}, and 5% C_{33}), we find $|\gamma_H|=|\gamma_D|=0.16$ eV. These various values for $n_0\gamma^2$ and $|\gamma|$ are shown in Tables II and III.

The same *temperature-independent* distribution of asymmetries was used to fit the data for both isotopes. The actual distribution may be temperature dependent. The distribution seen by a particular hydrogen ion depends on the occupancy of neighboring interstitial sites by other hydrogen ions. As the neighboring hydrogen ions become thermally excited with increasing temperature, the asymmetry seen by a particular ion may decrease. The shift of the distribution to smaller asymmetries with associated faster relaxation rates may be responsible for the strongly temperature-dependent rate required to fit our data.

V. CONCLUSIONS

Ultrasonic measurements in the 1-MHz range on $ScH_{0.25}$ and $ScD_{0.18}$ show attenuation peaks below 100 K: For $ScH_{0.25}$ the maximum attenuation occurs near 25 K; for $ScD_{0.18}$ the maximum occurs near 50 K. The general features of the results as well as the parameters used in fitting the data suggest that the motion seen in the ultrasonic experiments is closely related to that seen in NMR experiments. The results for both isotopes were fit with a TLS model involving tunneling between highly asymmetric sites. The relaxation of the TLS was fit as a sum of the two terms: τ_e^{-1}, probably due to coupling to electrons, and τ_p^{-1}, attributed to multiphonon processes. The rate τ_p^{-1} was 50 times stronger for $ScH_{0.25}$ than for $ScD_{0.18}$, in accordance with the idea that the relaxation involves tunneling. A surprising and unexplained result was that the rate τ_e^{-1} required to fit the data was the *same* for the two isotopes.

The dependence of the attenuation on the vibrational eigenmode and the observation of large attenuation peaks for vibrational eigenmodes involving only ε_4 and ε_6 shear motion indicate that the coupling of the TLS to the ultrasonic vibrations is due to a modulation of H-H (D-D) interactions between ions lying on parallel c axes. Ion pairs likely having a major role in this coupling were identified. With the assumption that the same fraction of hydrogen ions contribute to the ultrasonic attenuation in the two samples, we find that $|\gamma_H|\approx|\gamma_D|$; i.e., the coupling of the TLS to the ultrasound is isotope independent.

ACKNOWLEDGMENTS

R. G. Leisure is supported by Research Corporation. Ames Laboratory is operated for the U.S. Department of Energy by Iowa State University under Contract No. W-7405-Eng-82.

[1]J. P. Burger, J. N. Daou, A. Lucasson, P. Lucasson, and P. Vajda, Z. Phys. Chem. Neue Folge **143**, 111 (1985).
[2]C. K. Saw, B. J. Beaudry, and C. Stassis, Phys. Rev. B **27**, 7013 (1983).
[3]O. Blaschko, G. Krexner, J. N. Daou, and P. Vajda, Phys. Rev. Lett. **55**, 2876 (1985).
[4]M. W. McKergow, D. K. Ross, J. E. Bonnet, I. S. Anderson, and O. Schärpf, J. Phys. C **20**, 1909 (1985).
[5]O. Blaschko, G. Krexner, J. Pleschiutschnig, G. Ernst, J. N. Daou, and P. Vajda, Phys. Rev. B **39**, 5605 (1989).
[6]O. Blaschko, J. Pleschiutschnig, P. Vajda, J. P. Burger, and J. N. Daou, Phys. Rev. B **40**, 5344 (1989).
[7]O. Blascho, J. Less-Common Met. **172-174**, 237 (1991).
[8]I. S. Anderson, J. J. Rush, T. Udovic, and J. M. Rowe, Phys. Rev. Lett. **57**, 2822 (1986).
[9]T. J. Udovic, J. J. Rush, I. S. Anderson, and R. G. Barnes,

Phys. Rev. B **41**, 3460 (1990).
[10]J. Völkl, H. Wipf, B. J. Beaudry, and K. A. Gschneidner, Jr., Phys. Status Solidi B **144**, 315 (1987).
[11]I. S. Anderson, A. Heidemann, J. E. Bonnet, D. K. Ross, S. K. P. Wilson, and M. W. McKergow, J. Less-Common. Met. **101**, 405 (1984).
[12]J-W. Han, C-T. Chang, D. R. Torgeson, E. F. W. Seymour, and R. G. Barnes, Phys. Rev. **36**, 615 (1987).
[13]P. Vajda, J. N. Daou, P. Moser, and P. Rémy, Solid State Commun. **79**, 383 (1991); J. Phys. Condens. Matter **2**, 3885 (1990); P. Vajda, J. N. Daou, and P. Moser, J. Phys. (Paris) **44**, 543 (1983).
[14]I. S. Anderson, D. K. Ross, and J. E. Bonnet, Z. Phys. Chem. Neue Folge **164**, S923 (1989).
[15]I. S. Anderson, N. F. Berk, J. J. Rush, T. J. Udovic, R. G. Barnes, A. Magerl, and D. Richter, Phys. Rev. Lett. **65**, 1439 (1990).
[16]L. R. Lichty, J-W. Han, R. Ibanez-Meier, D. R. Torgeson, R. G. Barnes, E. F. W. Seymour, and C. A. Scholl, Phys. Rev. B **39**, 2012 (1989).
[17]I. Svare, D. R. Torgeson, and F. Borsa, Phys. Rev. B **43**, 7448 (1991).
[18]G. Cannelli, R. Cantelli, F. Cordero, F. Trequattrini, I. S. Anderson, and J. J. Rush, Phys. Rev. Lett. **67**, 2682 (1991).
[19]K. R. Maschhoff, E. Drescher-Krasicka, and A. V. Granato, in *Phonon Scattering in Condensed Matter,* edited by J. P. Wolfe and A. C. Anderson (Springer-Verlag, Berlin, 1986).
[20]G. Cannelli, R. Cantelli, and F. Cordero, Phys. Rev. B **34**, 7721 (1986).
[21]W. Morr, A. Müller, G. Weiss, H. Wipf, and B. Golding, Phys. Rev. Lett. **63**, 2084 (1989).
[22]R. G. Leisure, R. B. Schwarz, A. Migliori, D. R. Torgenson, I. Svare, and I. S. Anderson, in *Proceedings of the International Conference on Metal-Hydrogen Systems, Uppsala, Sweden, 1992* [Z. Phys. Chem. (to be published)].
[23]A. Migliori, W. M. Visscher, S. Wong, S. E. Brown, I. Tanaka, H. Kojima, and P. B. Allen, Phys. Rev. Lett. **64**, 2408 (1990).
[24]W. M. Visscher, A. Migliori, T. M. Bell, and R. A. Reinert, J. Acoust. Soc. Am. **90**, 2154 (1991).
[25]J. N. Daou, P. Vajda, A. Lucasson, and P. Lucasson, J. Phys. C **14**, 3155 (1981). J. E. Bonnet, C. Juckum, and P. Lucasson, J. Phys. F **12**, 699 (1983).
[26]J. Jäckle, Z. Phys. **257**, 212 (1972).
[27]S. Hunklinger and W. Arnold, in *Physical Acoustics,* edited by W. P. Mason and R. N. Thurston (Academic, New York, 1976), Vol. XII, p. 155.
[28]R. G. Leisure, R. B. Schwarz, A. Migliori, D. R. Torgeson, I. Svare, and I. S. Anderson, preceding paper, Phys. Rev. B **48**, 887 (1993).
[29]O. Blaschko, J. Pleschiutschnig, L. Pintschovius, J. P. Burger, J. N. Daou, and P. Vajda, Phys. Rev. B **40**, 907 (1989).
[30]Yu. Kagan, J. Low Temp. Phys. **87**, 507 (1992).
[31]W. A. Phillips, Rep. Prog. Phys. **50**, 1657 (1987).
[32]J. Kondo, Physica B **141**, 305 (1986).
[33]H. Grabert and U. Weiss, Phys. Rev. Lett. **54**, 1605 (1985).
[34]U. Weiss and M. Wollensak, Phys. Rev. Lett. **62**, 1663 (1989).
[35]Yu. Kagan and N. V. Prokof'ev, Zh. Eksp. Teor. Fiz. **97**, 1698 (1990) [Sov. Phys. JETP **70**, 957 (1990)].
[36]P. Doussineau, C. Frénois, R. G. Leisure, A. Levelut, and J.-Y. Prieur, J. Phys. (Paris) **41**, 1193 (1980).
[37]I. Svare, Physica **145B**, 281 (1987).
[38]F. M. Mazzolai, P. G. Bordoni, and F. A. Lewis, J. Phys. F **11**, 781 (1981).
[39]R. G. Leisure, T. Kanashiro, P. C. Riedi, and D. K. Hsu, Phys. Rev. B **27**, 4872 (1983).